Turkish Journal of Earth Sciences
http://journals.tubitak.gov.tr/earth/
Research Article
Turkish J Earth Sci
(2014) 23: 495-512

doi:10.3906/yer-1404-2

# Antique quarries of marmor troadense (NW Turkey): insights from field mapping and absolute dating

**Enver Vural YAVUZ***
Geology Engineering Department, Mining Faculty, İstanbul Technical University, İstanbul, Turkey

**Received:** 03.04.2014 • **Accepted:** 13.06.2014 • **Published Online:** 01.09.2014 • **Printed:** 30.09.2014

**Abstract:** In this study, we present new field and chronological data from 2 antique quarries of marmor troadense (Kestanbol quartz-monzonite) in northwestern Turkey. Marmor troadense has been mined and the building stones have been exported all over the Mediterranean region since approximately 2500 years ago. Analysis of 11 samples from the quarried bedrock for cosmogenic $^{10}$Be showed that the landscape is so old that the inheritance obscured the absolute dating of the operation periods. Nonetheless, $^{14}$C analysis of 4 charcoal samples from the sediments covering the ruins of Alexandria Troas indicated that these quarries stopped operating no later than 395 AD. These lines of evidence are in accordance with the results of field mapping. First, we mapped Kestanbol quartz-monzonite in detail and prepared a detailed geoarchaeological map of the quarrying activity in this area. We estimated the excavated amount of rock in 2 quarries to be >750 m$^3$ and identified 60 columns of granite and other building stones. Our findings suggest a gross budget of approximately 150 million euros for the quarry operations in this region based on present costs. Various operation periods of this large economy, if present, still remain to be uncovered.

**Key words:** Geoarchaeology, surface exposure dating, cosmogenic, $^{10}$Be, Kestanbol, Alexandra Troas, Neandreia

## 1. Introduction

The Kestanbol Intrusion, found as an outcrop in the Ezine village of Çanakkale (Figure 1), has been excavated for the production and export of building stones since ancient times (Ponti, 1995). For instance, the Romans traded Kestanbol quartz-monzonite (marmor troadense) all over the Mediterranean region (Lazzarini, 1987). Today, ruins of abandoned quarries where marmor troadense was once produced are found mainly in the area between Neandreia (built upon Çığrı Dağ Mountain) and the harbor city of Alexandria Troas (Feuser, 2009).

In these ruins, the size of the building stones varies from pavement stones to 12-m-long columns. The ruins of Alexandria Troas have also been called "Antigoneia", "Eski İstanbul" or "Eski Istamboul" (Choiseul-Gouffier, 1782; Cassas, 1786; Ricl, 1997), meaning "Old İstanbul", in medieval times, on old maps, and even still by locals. The ruins border the modern-day village of Dalyan to the north, on the Aegean coast in West Turkey (Figure 1). Alexandria Troas covers an area of approximately 400 ha with an approximately 7.1-km-long city wall (Choiseul-Gouffier, 1782; Wilson Jones, 1989; Schwertheim and Wiegartz, 1994; Ricl, 1997; Feuser, 2009). The death of Alexander the Great marked the beginning of the "Hellenistic Age", which ended with the defeat of the last Macedonian Kingdom, Ptolemaic Egypt, by the Romans (Errington, 2008), or, more precisely, the defeat of Antony and Cleopatra by Octavian in 31 BC (Green, 2007). The Hellenistic Period brought fundamental changes to the ancient world on a scale never seen before (Green, 2007). After the death of the Macedonian King Alexander the Great, his empire, stretching from the Aegean to the Punjab region, fragmented under the struggle among his officers longing for power (Errington, 2008). The empire was divided into several provinces and ruled by the successors of Alexander the Great, each trying to overpower the others by force or influence (Green, 2007). Among the successors were Antigonus, Lysimachus, and Seleucus, who contributed greatly to the development of Alexandria Troas. Reorganization and union of mainly autonomous Greek communities took place during this time along the Aegean coastline, which rose in importance and flourished (Errington, 2008). The foundation of Alexandria Troas lies in the period of reorganization, which followed the struggles among the successors of Alexander the Great and the Roman claim of power over the Greek territory. Alexandria Troas was conceived as a trading center connecting its hinterland to the rest of the ancient world through its harbor (see Feuser, 2009, for further details).

* Correspondence: vural@itu.edu.tr

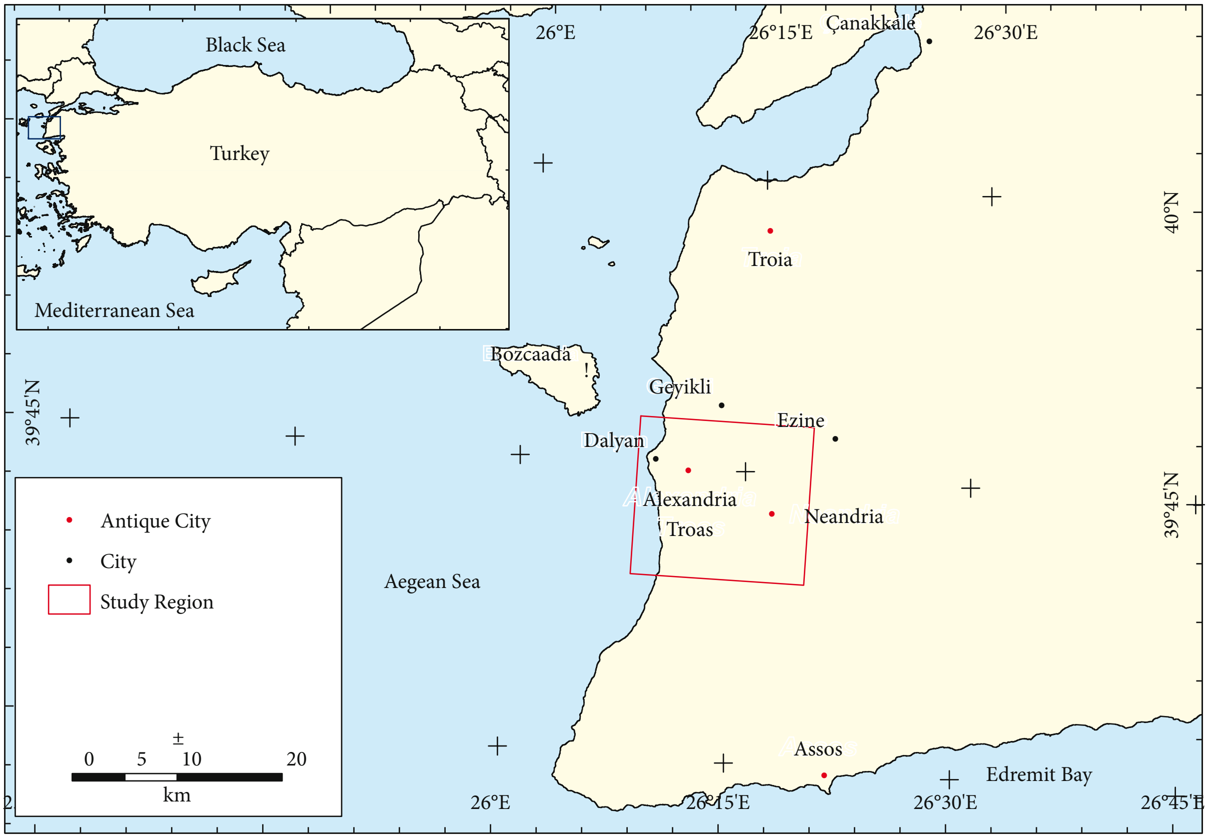


**Figure 1.** Location of the study area in Northwest Turkey. Red inset shows the extent of the geological map in Figure 2. Ancient cities are given in italics and marked with red dots, whereas modern cities are with black dots.

The ancient city of Neandreia is located at the highest point of the study area, Çığrı Dağ (Figure 1). This city is approximately 12 km SE of Alexandria Troas and 10 km from the Aegean Sea. Neandreia covers an area of 1400 × 450 m and is surrounded by a 3-m-thick city wall with a length of 3.2 km (Koldewey, 1891). The first traveler to visit Neandreia was Pococke (1743–1745), but he called the city Chigur, with an uncertain identification. Similarly, other travelers (e.g., Virchow, 1879) misinterpreted the city on Çığrı Dağ to be Kenchreai. Only Clarke (1886) proved that this city was Neandreia. During Prehistoric or Neolithic times, a first settlement on top of Çığrı Dağ could have existed, based on a single, superficial flint stone finding by Schwertheim and Wiegartz (1994). However, this single finding cannot be regarded as proof of a culture. Mythological traditions put the early history of Neandreia into the dominion of Kyknos, Son of Poseidon, King of Kolonai, and father of the founder of Tenedos. Another tradition says that Kyknos, ruler of Neandreia, was helping the Trojans fighting with the Achaeans during the Trojan War in 1240 BC. The Achaeans killed Kyknos and conquered the Troas, including Neandreia. Thus, it seems likely that Neandreia already existed in the 2nd millennium BC. The Aeolians reorganized and renewed the city in the 8th or 7th century BC and are considered the real founders of Neandreia (Schwertheim and Wiegartz, 1994). Some dated findings from cist graves fall in this period (Koldewey, 1891). In the 6th century, the city was enlarged and an Apollon temple was built (Schwertheim and Wiegartz, 1994). The first wall system around Neandreia was most likely built in this context (Schulz, 2000). Neandreia was, at least from 454 to 431 BC, a part of the Delian-Attic Union (Schulz, 2000). Although, Neandreia was autonomous, it had little influence. Its economy consisted mainly of agriculture and horse breeding (Schwertheim and Wiegartz, 1994). Akarca (1977) suggested that the city wall collapsed from time to time and was reerected, as visible in the different styles of the construction work. At the end of the 5th century, Neandreia was affected by the struggles for power during the Persian wars and the Peloponnesian war. Subsequently, Neandreia fell into Persian hands and was ruled by Dardanos. After Dardanos' death, Mania, the wife of Zenis, became the ruler of Neandreia in 399 BC. During this period, Greek mercenary troops were accommodated at Neandreia (Schwertheim and Wiegartz, 1994). A second wall system dates back to approximately the 4th century BC;

therefore, it is possibly connected to Mania's reign (Schulz, 2000). Winter (1985) suggested that the construction of the second wall circuit dates to approximately 325 BC. Mania's son-in-law, Meidias, assassinated her soon afterwards. This led to rioting not only among troops and the population of Neandreia but also among Meidias' troops and troops loyal to Mania. Meidias could not manage to reign over Neandreia; instead, the military leader Derkylidas, who commanded the troops stationed at Neandreia, was more successful (Schwertheim and Wiegartz, 1994). During the process of synoecism, introduced by Antigonus Monophthalmus between 311 and 306 BC, the inhabitants of Neandreia and 7 other autonomous communities were transferred to the newly built Hellenistic city Alexandria Troas (Ricl, 1997). According to Winter (1985), this is the reason why no fundaments are found in the eastern part of Neandreia, because the inhabitants had no time between the erection of the second wall system and the synoecism to settle in this part. After the synoecism, Neandreia disappears from historical sources. Therefore, Koldewey (1891) thought that Neandreia was completely deserted. However, Schwertheim and Wiegartz (1994) and Ricl (1997) suspected that Neandreia was not completely deserted after the synoecism, though no more trading was done in Neandreia. They also suggested that a small number of the original inhabitants remained at Neandreia to maintain the vital water supply for the region between Troy and Antigoneia and to perform ancestral rituals cults and funeral rites for their dead, but they were not autonomous anymore. Furthermore, Schliemann (1881) and Cook (1959) suggested a Roman reoccupation in the region, possibly by military troops. Clarke (1886) assumed that not only Romans but also Goths, Armenians, and Franks claimed the site as their own. Both these theories have not been proven until today.

The quartz-monzonite of the Kestanbol Intrusion was known in ancient times as "marmor troadense" or "granito violetto" due to its slightly violet luster (Lazzarini, 2002). The first known usage of the quartz-monzonite was by the Aeolic Neandreians in building up their city wall with quartz-monzonite blocks. The columns and other building stones quarried from the Kestanbol Intrusion during Roman times were transported to the harbor of Alexandria Troas and exported over sea and land throughout the Mediterranean region (Lazzarini, 1987). The first use of such columns is suggested in Tivoli at the Piazza d'Oro and in the Ostia nel Foro (Lazzarini, 1987). The number of columns identified in the circum-Mediterranean area varies between 2 and 88 (Feuser, 2009). The total number of columns is not known, but 314 columns have been scientifically confirmed. However, this number covers only one-fourth of the mentioned locations. Therefore, 314 columns is by far the minimum number of exported columns.

During Roman times, as Lazzarini (1987) suggested, quarrying started in the 2nd century BC and lasted approximately until the 2nd century of the Byzantine Empire, corresponding to the 6th century AD. This hypothesis was also supported by Williams-Thorpe (2008). Pensabene (2002) said that quarries, during that time, were almost exclusively imperial ones. According to Ponti (1995), quartz-monzonite columns appeared in many imperial construction projects in Italy in the 2nd century BC, confirming Lazzarini's suggestion, but this fact gives no hint of early quarry activities during Roman times. Furthermore, Greeks did not often use granite for their constructions; they preferred softer marble. However, it cannot be ruled out that a transfer of knowledge about how to work with granite occurred between the Egyptians and the Troad (Galetti et al., 1992) around 2000 BC or even earlier (Waelkens, 1992). The quarries seem to have still been in use in 313 AD, because the replacement of old columns by quartz-monzonite columns is noted in an inscription from Leptis Magna for the restoration of the Forum Vetus. Text passages in the Theodosian Code, from the years 414 and 416 AD, mention the quarries in the Troad, implying that there was large-scale production during that time, possibly under imperial administration (Ponti, 1995). However, it remains unclear when exactly the quarrying of the Kestanbol Intrusion started during Roman times and when it was given up, due to missing inscriptions within the quarries or on the building stones themselves and to the lack of archaeological investigations and dating (e.g., no material for radiocarbon ages) (Ponti, 1995).

After the abandonment of the quarries, many of the previously produced building stones were reused by succeeding civilizations. It is known that, for example, the Ottomans removed marmor troadense building stones from the city wall, the ruins of Alexandria Troas, and other ancient cities to build the harbor of İstanbul or to produce catapult projectiles (Lazzarini, 1987). Another example of the use of Kestanbol quartz-monzonite columns is in the building of the Sultan Ahmet Mosque. In the reign of Sultan Mehmet IV, columns were used to build his mosque (or possibly the conversion of the Hagia Sophia). Hence, 2 ships were loaded each day with stones from the ruins of Alexandria Troas and transported to İstanbul (Taşçı, 2010). However, Taşçı did not indicate over what time span this transport took place. Although there is no record of quarrying activity during Byzantine or Ottoman times, it still cannot be completely ruled out. A complete list of primary and secondary destinations, due to such reuse, can be found in the work of Lazzarini (1987). According to Lazzarini (2004), marmor troadense is one of the most distributed building stones in antiquity. Other examples of locations where Kestanbol quartz-monzonite was used include Efesos along the Via Marmorea and Venice in the

Basilica di San Marco (Lazzarini, 1987). Not all columns and building stones were removed from the quarries. There are monolithic columns still lying in the deserted quarries. The most famous quarry of the area is the Yedi Taşlar quarry, among an unknown number of other quarries throughout the Kestanbol Intrusion, as described by Lazzarini (1987), Birkle and Satır (1994), and Ponti (1995).

At Yedi Taşlar, columns of approximately 11.5 m in length and 1.6 m in diameter (Ponti, 1995) were reported. Schliemann (1881) mentioned that 3 quartz-monzonite columns were found abandoned in the harbor of Alexandria Troas. The reason for the abandonment of these columns can only be speculated. However, it might be closely related with the fall of Alexandria Troas. According to Dworakowska (1983), few quarries remained intact over the centuries. Therefore, the excellent preservation of quarries in the Kestanbol Intrusion makes them extremely valuable for further investigations regarding quarries and quarrying technique in general.

In this study, we focus on the antique quarries of marmor troadense in the Troad (Figure 1). We mapped the Kestanbol intrusion around Neandreia in detail, with the aim of revealing the extent of these quarries. We also prepared a detailed geoarchaeological map of the antique quarries. To reconstruct the operational chronology of these quarries, 11 samples from the quarried bedrock and 4 charcoal samples from the sediments covering the ruins of Alexandria Troas were collected in field for cosmogenic $^{10}$Be analysis and $^{14}$C analyses, respectively. Our study enabled an estimation of gross revenue of approximately 150 million euros from quarrying, which is reflected in the wealth of Alexandria Troas. Although inheritance of $^{10}$Be inhibited the exposure dating of antique quarries, $^{14}$C dating indicates an age of approximately 400 AD for the simultaneous collapse of this economic system with Alexandria Troas.

## 2. Study area

The study area lies to the southwest of the Ezine village of Çanakkale on the Biga Peninsula in northwestern Anatolia, Turkey (Figure 1). In ancient times, this area belonged to Troas, which is delineated in the north by the Dardanelles, in the west by the Aegean Sea, and in the south by the Gulf of Edremit. Neandreia and Alexandria Troas are the ancient cities located in the study region. Although most of the Biga Peninsula has been declared an archaeological heritage site, archaeological excavations are concentrated in Troy, 30 km to the north of the study area. In the other sites, limited archaeological excavations have been conducted.

The geology of the study region is manifested by tectonics and magmatism (Savaşçin and Güleç, 1990; Seyitoğlu and Scott, 1996; Aldanmaz et al., 2000; Beccaletto, 2003; Altunkayanak and Genç, 2008; Figure 2). During the Permian, Anatolia was situated in the northernmost part of the Gondwana supercontinent (Şengör and Yılmaz, 1981). The formation of the Biga Peninsula commenced in the Middle Triassic, when the Cimmerian continental fragment split from the main continent and the southern branch of the Neotethys rifted. Ongoing fragmentation and rifting of the Cimmerian continent during the Early Jurassic resulted in the formation of the Anatolian-Tauride platform between the northern and southern Neotethys. The Cimmerian continent collided with Eurasia in the Middle Jurassic and caused uplift and the closure of the Paleo-Tethys (Şengör and Yılmaz, 1981). Beccaletto (2003) located the Biga Peninsula to the western part of the Sakarya Zone, which has a continental basement of metamorphic rocks of uncertain age as well as Devonian granitoids, as part of the Laurasian margin during the Jurassic and Late Cretaceous. The Karakaya Complex, a Triassic subduction and accretion complex, underlies the Mesozoic sequences. The Karakaya Complex consists of phyllite, eclogite, greywacke (paleogeographically, a seamount or oceanic plateau) and a mélange zone (paleogeographically, a forearc basin related to the Paleo-Tethys subduction along the southern margin of Eurasia) (Okay and Tüysüz, 1999; Beccaletto, 2003).

The main phase of magmatism in the Biga Peninsula occurred between the Eocene and Miocene. This magmatic phase was affected in early stages by asthenospheric upwelling induced by slab break-off and in later stages by subduction-derived fluids (Tethyan subduction dipping beneath the Sakarya Complex; Altunkaynak and Genç, 2008).

The main plutonic body in the study area is the Kestanbol Intrusion (Figure 2; Fytikas et al., 1976). This intrusion was followed by postcollisional extension starting in the Late Oligocene. At the same time, uplift of the Kazdağ massif, to the SE of the study region, took place in association with lithosphere thinning or delamination of subcontinental lithospheric mantle. Both the extension and the uplift led to the next phase of magmatism and volcanism in the region (Altunkaynak and Genç, 2008).

The first detailed description of the complex tectonic activity of the Biga Peninsula was provided by Philippson (1918). More recent overviews were given by Bingöl (1976), Okay and Tüysüz (1999), Bozkurt (2001), and many others. Yılmaz and Karacık (2001) suggest an Early Miocene, NNE trending fracture and fault system causing the deposition of pyroclastic rocks and intermediate lavas on the top of lake sediments. During the Middle Miocene, a compressional regime followed by a N-S extensional regime in the Upper Miocene created NE-SW trending horst-graben structures with major strike-slip displacements.

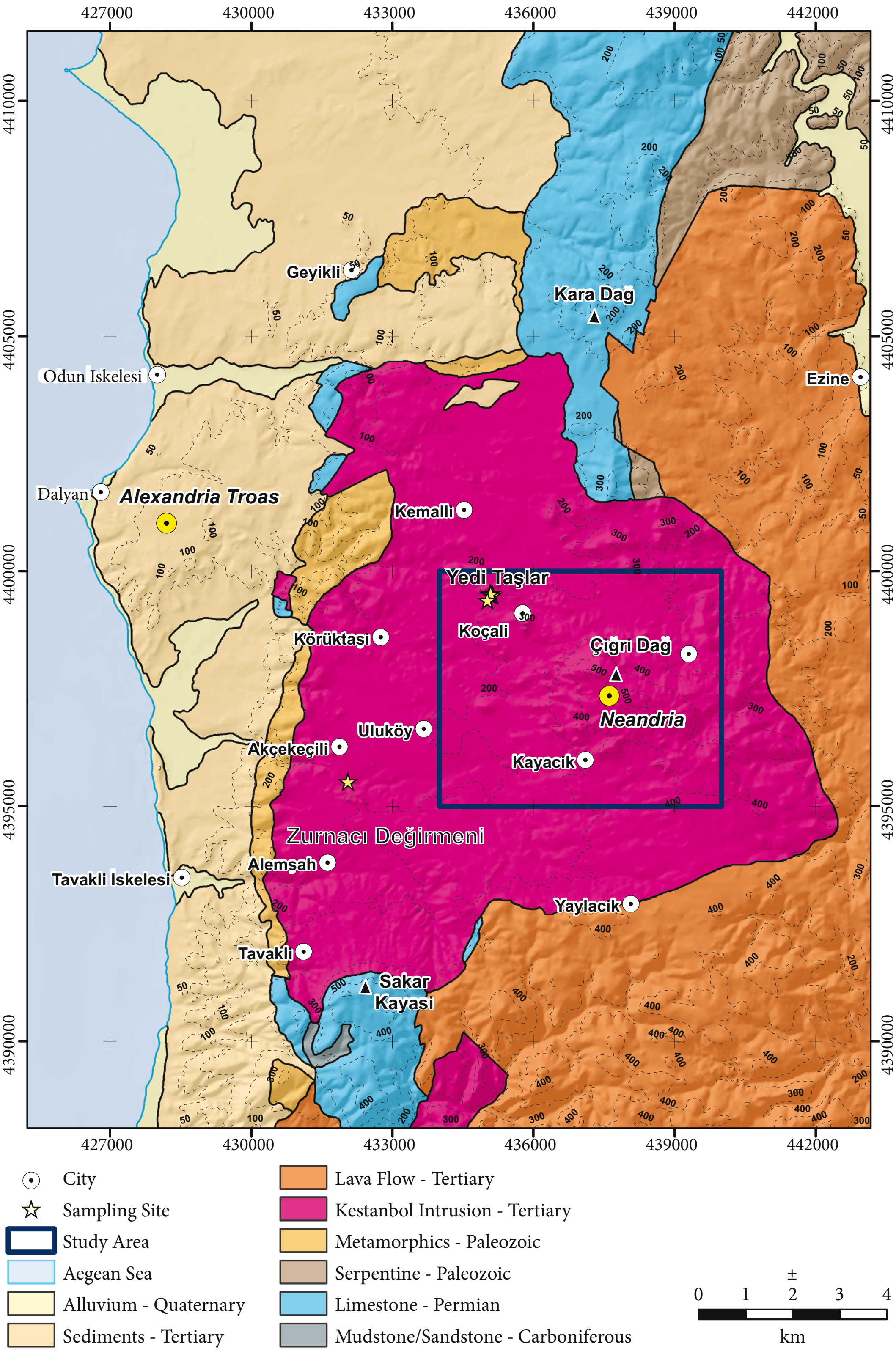


**Figure 2.** Geological map of the study region (modified after Mützenberg, 1991).

In our study area, several NE-SW trending fracture zones, considered branches of the Gülpınar Fault Zone, are still active and directly connected to hydrothermal activity, e.g., hydrothermal springs (Mützenberg, 1991; Çağlar and Demirörer, 1999). During the Pliocene and Quaternary, the prior horst-graben system was overprinted by an E-W horst-graben system (Yılmaz and Karacık, 2001). The cause of the mentioned extensional tectonic is debatable. Several suggestions have been made, which include tectonic escape (shortening caused by partial closure of the Neotethys), back-arc spreading (migration of the trench system of the subduction in the Hellenic arc), and orogenic collapse (simultaneous orogenic collapse and start of roll-back process) (Seyitoğlu and Scott, 1996).

The Late Quaternary landscape evolution of the Biga Peninsula can be summarized in 3 distinct phases (Kayan, 1999, and references therein). The first is the postglacial transgression and the resulting aggradation during the Early Holocene. The second is the end of sea-level rise after reaching the present level during the Middle Holocene, besides the small-scale oscillations. Fluvial progradation dominated this transition from marine to terrestrial environment. The third and final phase is the end of this progradation during the Late Holocene, when delta plains were covered by flood plain deposits (Kayan, 1999, and references therein).

The Kestanbol Intrusion outcrops are found in Ezine village (Figure 2). The surficial extent of the Kestanbol Intrusion is 80 to 100 km$^2$, which builds a plateau between 100 and 300 m above sea level (Mützenberg, 1991; Birkle and Satır, 1994). Çığrı Dağ represents the highest point with an elevation of 529 m above sea level. According to Mützenberg (1991), the Kestanbol Intrusion consists almost exclusively of biotite- and hornblende-bearing quartz-monzonite. The Kestanbol Intrusion is one of the most homogeneous intrusions globally. Spühler (1991) mentioned hydrothermal copper, lead, and zinc ore deposits around Aladağ. Here, magnetite was the main mineral to be exploited, but galenite, sphalerite, hematite, and chalcosine are also found. The intrusion is surrounded by Paleozoic metamorphic rocks, Paleozoic serpentinites, Permian limestones, Tertiary lavas, Tertiary sediments, and Quaternary alluvial deposits (Figure 2; Mützenberg, 1991). Skarn formation is reported at the contact between limestones and metamorphic limestone-silicate schists. The ore deposits along the northern contact of the Kestanbol intrusion seem likely to be associated with the skarn formation (Spühler, 1991). Fytikas et al. (1976) determined a K/Ar age of 28 ± 0.88 Ma for the Kestanbol Intrusion, while Delaloye and Bingöl (2000) obtained a K/Ar age of 20.5 ± 0.6 Ma. Furthermore, Birkle and Satır (1994) obtained an Rb/Sr cooling age of 21 ± 2 Ma for the same intrusion.

## 3. Methodology

In this study, 8 samples from excavated bedrock surfaces in the Yedi Taşlar Antique Quarry, 2 samples from the excavation steps in the Zurnacı Değirmeni Antique Quarry, and 1 from the bedrock of the Yedi Taşlar Antique Quarry were collected with a hammer and chisel (after Akçar et al., 2011) for cosmogenic $^{10}$Be analysis. Geographical positions and details of the samples are presented in Table 1. In addition to the bedrock samples, 4 charcoal samples were also collected from the sediments overlying the ruins of Alexandria Troas for radiocarbon dating.

Bedrock samples for $^{10}$Be analysis were processed at the Surface Exposure Dating Laboratory of the University of Bern. Following the protocol of Akçar et al. (2012), samples were crushed and sieved to size fractions of 0.25–0.5 mm. The nonmagnetic fractions were separated using a Franz isodynamic magnetic separator. Quartz was purified following a modified version of the Kohl and Nishiizumi method (Kohl and Nishiizumi, 1992; Akçar, 2006). Be was extracted according to Akçar et al. (2012) and prepared for accelerator mass spectrometry (AMS) measurements at the ETH Laboratory of Ion Beam Physics. The $^{10}$Be/$^{9}$Be ratios were normalized to ETH in-house standard S2007N (Kubik and Christl, 2010) based on the $^{10}$Be half-life of 1.387 Ma (Chmeleff et al., 2010; Korschinek et al., 2010). A full process blank ratio of (3.34 ± 0.56) × $10^{-15}$ was subtracted from the measured ratios and the error was propagated accordingly. Cosmogenic nuclide data for the samples are presented in Table 2. $^{10}$Be exposure ages were calculated with the CRONUS-Earth online calculator of Balco et al. (2008; http://hess.ess. washington.edu/math/) using the NE North American production rate calibration dataset (Balco et al., 2009; wrapper script 2.2, main calculator 2.1, constants 2.2.1, and muons 1.1). The shielding of the surrounding topography is based on Dunne et al. (1999) and the thickness of the sample using an exponential attenuation length of 160 g/cm$^2$ was accounted for calculating $^{10}$Be exposure ages (Table 1). No correction for erosion, snow, or vegetation was applied.

Charcoal samples were chemically treated and graphitized at the ETH Laboratory of Ion Beam Physics for the AMS analysis. Radiocarbon ages were calibrated to OxCal 3.1 (https://c14.arch.ox.ac.uk/oxcal; Ramsey, 2005) using atmospheric data from Reimer et al. (2009).

## 4. Results

An area of approximately 30 km$^2$, between Bekçitaşı Hill to the north, Yavaşlar village to the west, Kayacık village to the south, and Ulaç Hill to the east, was mapped in the field (Figure 3). Neandreia is located at the center of our study area and sits enthroned on the top of Çığrı Dağ. From there, one can view the surrounding area, including the land where Alexandria Troas was located and the island of Bozcaada on the horizon.

**Table 1.** Description of the samples from the antique quarries.

| Sample name | Quarry | Altitude (m a.s.l.) | Latitude, °N (DD.DD) | Longitude, °E (DD.DD) | Sample thickness (cm) | Thickness correction factor[b] | Shielding correction factor[c] |
|---|---|---|---|---|---|---|---|
| T-1A | Yedi Taşlar | 216 | 39.7414 | 26.2417 | 4.0 | 0.9670 | 0.6259 |
| T-2 | | 216 | 39.7414 | 26.2417 | 5.0 | 0.9590 | 0.6259 |
| T-3 | | 220 | 39.7414 | 26.2418 | 2.0 | 0.9833 | 0.7096 |
| T-4 | | 219 | 39.7413 | 26.2422 | 3.0 | 0.9751 | 0.5723 |
| T-5 | | 218 | 39.7414 | 26.2418 | 5.0 | 0.9590 | 0.6259 |
| T-6 | | 214 | 39.7414 | 26.2416 | 4.0 | 0.9670 | 0.6259 |
| T-7 | | 224 | 39.7413 | 26.2423 | 4.0 | 0.9670 | 0.9982 |
| [a]T-8 | | 237 | 39.7415 | 26.2419 | 5.0 | 0.9590 | 1.0000 |
| T-9 | | 205 | 39.7402 | 26.2411 | 5.0 | 0.9590 | 0.5000 |
| T-10 | Zurnacı Değirmeni | 154 | 39.7053 | 26.2087 | 5.0 | 0.9590 | 0.9700 |
| T-11 | | 156 | 39.7053 | 26.2087 | 4.5 | 0.9630 | 0.9898 |

[a] Bedrock sample.
[b] Calculated for sample thickness with an uncertainty of ±0.5 cm after Gosse and Phillips (2001), with mean attenuation length of 160 g/cm$^2$ and rock density of 2.65 g/cm$^3$.
[c] Calculated for topographic shielding and dip of the surface after Dunne et al. (1999).

**Table 2.** Cosmogenic nuclide data of samples from the antique quarries.

| Sample name | Quarry | Quartz dissolved (g) | $^9$Be spike (mg) | $^{10}$Be ($10^4$ at/g) | | | Apparent exposure age (ka) | | | |
|---|---|---|---|---|---|---|---|---|---|---|
| T-1A | Yedi Taşlar | 52.5198 | 0.2025 | 1.93 | ± | 0.21 | 6.8 | ± | 0.7 | (0.8) |
| T-2 | | 34.5677 | 0.2031 | n.a. | | | | | | |
| T-3 | | 78.7123 | 0.2278 | 2.41 | ± | 0.13 | 7.3 | ± | 0.4 | (0.5) |
| T-4 | | 101.0197 | 0.2183 | 2.00 | ± | 0.10 | 7.5 | ± | 0.4 | (0.5) |
| T-5 | | 102.6465 | 0.2543 | n.a. | | | | | | |
| T-6 | | 107.2270 | 0.2236 | 2.33 | ± | 0.11 | 8.2 | ± | 0.4 | (0.6) |
| T-7 | | 102.6756 | 0.2540 | 4.88 | ± | 0.24 | 10.9 | ± | 0.5 | (0.8) |
| [a]T-8 | | 83.8621 | 0.2275 | 59.38 | ± | 1.78 | 130.4 | ± | 4.2 | (7.7) |
| T-9 | | 71.4002 | 0.1744 | 2.19 | ± | 0.18 | 9.6 | ± | 0.8 | (0.9) |
| T-10 | Zurnacı Değirmeni | 86.7962 | 0.1723 | 1.94 | ± | 0.09 | 4.8 | ± | 0.2 | (0.3) |
| T-11 | | 90.5257 | 0.1746 | 2.53 | ± | 0.11 | 6.1 | ± | 0.3 | (0.4) |

[a] Bedrock sample.
Note: AAD measurement errors are at the 1 α level, including the statistical (counting) error and the error due to normalization of standards and blanks. The error weighted average $^{10}$Be/$^9$Be full process blank ratio is (2.84 ± 0.29) × $10^{-15}$. Exposure ages are calculated with the CRONUS-Earth exposure age calculator (http://hess.ess.washington.edu/math/; v. 2.2; Balco et al., 2008 and update from v. 2.1 to v. 2.2 published by Balco in October 2009) and time-dependent Lal (1991)/Stone (2000) scaling model using the NE North American production rate calibration dataset (Balco et al., 2009). Exposure ages are corrected for dip of rock surface, shielding of surrounding topography, and sample thickness, as explained in the text; the uncertainties reported in parentheses also include the production rate error. For age calculations, 2.65 g/cm$^3$ for rock density and a half-life of 1.39 Ma for $^{10}$Be (Korschinek et al., 2010; Chmeleff et al., 2010) are used.

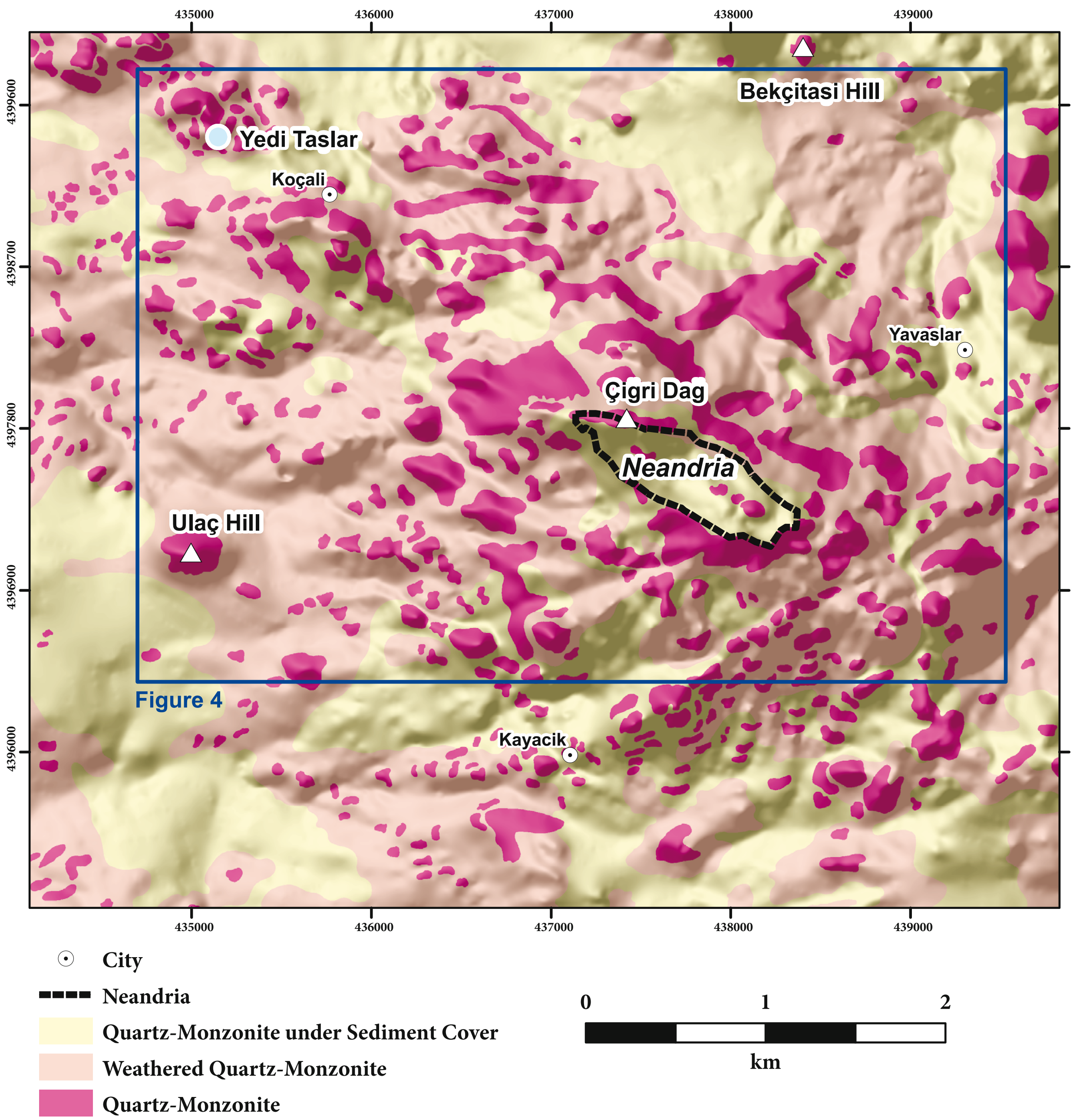


**Figure 3.** Detailed geological map of the study area. Inset shows the extent of Figure 4.

The Kestanbol Intrusion was mapped into 3 units: (1) quartz-monzonite bedrock, (2) strongly weathered quartz-monzonite, and (3) quartz-monzonite covered by Quaternary sediments (Figure 3). The main part of the bedrock outcrops of the Kestanbol Intrusion consists of biotite and hornblende-bearing quartz-monzonite, which is very homogeneous in its composition (Lazzarini, 1987; Mützenberg, 1991; Galetti, 1992). At a macroscopic scale, xenolithic mafic clasts are abundant. The xenoliths have feldspar and biotite phenocrystals in a fine-grained matrix composed of biotite, plagioclase, and hornblende. It can be assumed that these xenoliths are partially molten relicts of the surrounding rock. Porphyroclastic feldspars are slightly orientated. Another macroscopic observation about the top samples is that they usually show stronger weathering characteristics, which is seen in the formation of clay minerals. The quartz-monzonite in the study area has a hypidiomorphic and holocrystalline texture. No deformations are visible at the macro- or microscopic scale. Porphyroclastic feldspars are embedded in a coarsegrained matrix consisting of plagioclase, hornblende, biotite, quartz, pyroxene, magnetite, and titanite, listed here in order of decreasing abundance. All minerals except feldspars and quartz act also as inclusions.

Strongly weathered bedrock in the area represents the second unit of our map. Spheroidal weathering or woolsack weathering is a typical feature of granitic or quartz-monzonitic rocks (Birkle and Satır, 1994), where rounded blocks are surrounded by disintegrated landscape. Blocks are still connected with their bedrock in most cases, no matter how strongly their surrounding has disintegrated.

We also classified spheroidal blocks and "onion shale" peel-off (Birkle and Satır, 1994) structures in the "strongly-weathered bedrock" unit. In some blocks, tafoni and honeycomb weathering structures form the basis of the hanging wall, while lateral blocks showing lateral tafoni and honeycomb weathering structures represent rotated blocks. Based on their shapes, these lateral structures are also inferred to have formed on the former hanging part. The landscapes of the mapped area do not show equal disintegration in all parts. In stable core regions of the intrusion such as, for example, Çığrı Dağ, the bedrock is less disintegrated. However, the outcropping quartz-monzonite is rounded on top and shows frequent "onion shale" peeling-off of the outermost rock cover.

The last unit of our geological map is the quartz-monzonite covered by Quaternary sediments. These deposits are generally thin; for instance, a sediment cover with regolith formation of 40 cm was measured along a road cut.

In addition to the detailed geological map, a detailed geoarchaeological map was also produced in the field to investigate the evidence for ancient quarry operation. Columns, rectangular building stones, chiseling chips, old transport paths, and quarries were mapped in detail, and the extent of the quarries in an area of 3.7 km$^2$ was determined for this purpose (Figure 4).

Quarries in our mapping area are highly variable in size. The most famous and most likely the biggest quarry of the Kestanbol Intrusion is the Yedi Taşlar Quarry. The extracted volume of rock is at least 600 m$^3$ but could be much more, due to the unknown amount of debris filling

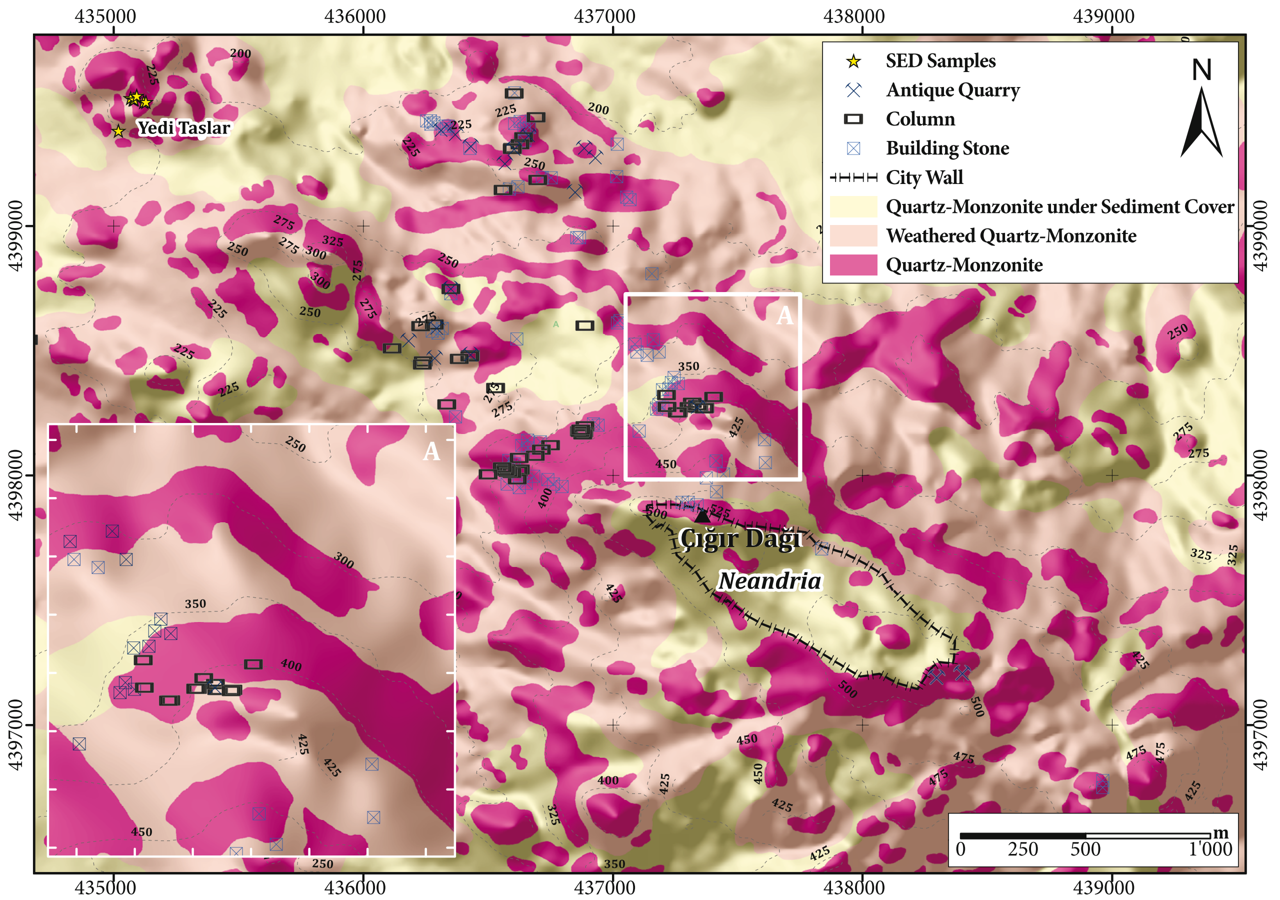


**Figure 4.** Geoarchaeological map of the area around Neandreia. Insets are close-up views to show the details of the mapped features (modified from Haudenschild, 2011).

up the quarry. From field observations, we infer that the initial ground level must have been deeper than today's, which is also true for other quarries in the study area. The volume of excavated rock in the mapped quarries varies from 4 to approximately 150 $m^3$. Most quarries show different working steps. The height of a single working step varies from 30 to 1.30 cm according to the produced building stones for every quarry. The smaller steps usually were used to produce rectangular blocks or small columns, while bigger steps led to bigger columns. Quarries are distributed all over the mapped area, except the direct surrounding of Neandreia. Some quarries are on top of mountain ridges surrounded by steep slopes, while others are located on hillocks. Compact boulders were also quarried.

Sixty columns and column fragments were mapped of different sizes, in different stages of work progress, and with different preservations. Some columns were ready for transport while some were partly ready, and others were still in situ and in some cases were connected to the bedrock. There are many fragmented columns, with pedestal rocks interspersed throughout. To be sure that a particular fragment or a pedestal is examined, further investigations and excavations would be necessary because in most cases only the upper part with the collar is visible at the surface. The remaining parts might be broken or completely covered by sediments. Columns are, except for Neandreia, distributed all over the mapping area (Figure 4). Completed columns usually have a collar, which is thicker than the actual shaft, on both ends; sometimes a 2-tiered collar is also observed on an end. In a few cases, the outline of the collar was already marked on row-stage columns.

Column lengths vary from 40 to 570 cm. A length of up to 50 cm is the most common length type in the mapped area. However, most of these are broken column pieces or pedestals. From 180 cm upwards, the columns are complete in length. Wherever fragmented pieces were lying next to each other belonging to the same piece, the total length was measured. It can be concluded that, in the mapping area, broken column fragments make up the biggest part of the identified columns, followed by columns of 151 to 250 cm. No columns as long as the ones in Yedi Taşlar or in the Quarry near Zurnacı Değirmeni (12 m) were found in the study area. The columns can be sorted into 3 groups according to Barresi (2002). Bigger columns of ca. 12 m or more are not available, as in Yedi Taşlar. However, we mapped some columns of intermediate length (~4 m). We classify columns between 3 and 6 m as being of intermediate size. However, as described above, the majority of columns are less than 3 m long and therefore belong to the category of small columns. A broad variability in the diameters of the columns is also visible. In general, the column width tapers towards the top. Therefore, 2 measurements of diameters at the foot and at the top were taken whenever possible. In the mapped area, diameters of the columns vary from 30 to 100 cm with the longest columns in the Kestanbol Intrusion being 1.6 m thick (e.g., at Yedi Taşlar). By far, most of the columns in the mapping area are between 50 and 60 cm in diameter. According to Barresi (2002), Roman columns usually have a 1:8 ratio of length to diameter.

However, in the study area, only a few columns agree with Barresi's ratio. Most of these columns have a ratio of between 1:4 and 1:5, as well as 1:6 and 1:8. Barresi's 1:8 ratio can be supported if the ratios of the Yedi Taşlar columns are also considered.

Yedi Taşlar is 8.8 km east of the harbor of Alexandria Troas and approximately 830 m west-northwest of Koçali (Figure 4). Samples T-1 to T-7 were taken in 2008 from different Roman working steps, each corresponding to a different level of excavation (Figure 5). T-9 is not visible in Figure 5 as it is located 100 m southeast of Yedi Taşlar. To investigate the minimum age of the landscape, sample T-8 from the top of the quartz-monzonite outcrop was collected. The field observations rule out any human impact at this location. Approximately 5 km south-southwest of Yedi Taşlar, 8 km south-southeast of the harbor of Alexandria Troas (to where the completed columns were transported), and close to the village Akçekeçili (Figure 2), 2 different working steps at 2-m vertical distances to each other were sampled in 2009 (Figure 6).

For each sample, the amount of the dissolved quartz, $^{9}Be$ spike, $^{10}Be$ concentration, and apparent exposure ages are reported in Table 2. The 1-s uncertainties that include the production rate error are presented in parentheses. The corrections to account for thickness, dip of rock

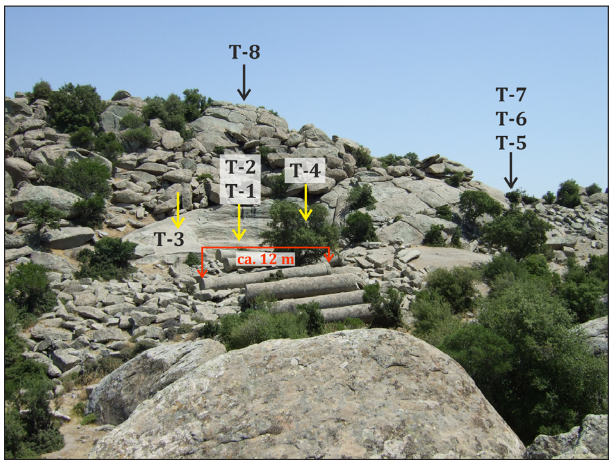


**Figure 5.** Ruins of the Yedi Taşlar Antique Quarry and sample locations. Note that T-8 is collected from a natural bedrock surface.


**Figure 6.** Sampled excavation steps in ruins of the Zurnacı Değirmeni Antique Quarry.

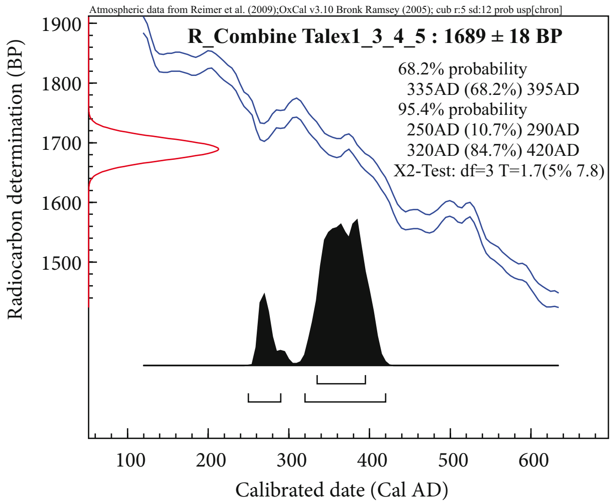


**Figure 7.** Combined radiocarbon calibration for the charcoal samples.

surface, and shielding of the surrounding topography were included in the calculation of exposure ages, but erosion and snow correction were excluded. We use apparent exposure ages with uncertainties including the production rate errors for our discussion.

Bedrock sample T-8 yielded a $^{10}$Be concentration of (59.38 ± 1.78) × $10^4$ at/g and an exposure age of 130.4 ± 7.7 ka (Table 2). Due to the high total Al concentrations, AMS measurements of samples T-2 and T-5 were not successfully completed. $^{10}$Be concentrations of the other samples vary between (1.94 ± 0.09) × $10^4$ and (4.88 ± 0.24) × $10^4$ at/g. For these samples, apparent ages from 4.8 ± 0.3 ka to 10.9 ± 0.8 ka were calculated (Table 2).

The analysis of charcoal samples from the sediments covering the ruins of Alexandria Troas yielded a $^{14}$C age of 1689 ± 18 BP (Figure 7; Table 3). The calibration indicated that the collapse of Alexandria Troas occurred between 335 and 395 AD within 2-s uncertainty. This age fits well with the period in which the last records of Alexandria Troas appear in ancient literature. Bishop Silvanus and Bishop Pionius visited Alexandria Troas in 420 AD and 451 AD, respectively (Ricl, 1997). Based on the calibrated $^{14}$C age and the ancient literature, it can be inferred that some parts of Alexandria Troas was already destroyed and possibly also deserted by that time. Therefore, 395 AD is taken as the last period when the quarry operations were active in the study area. Based on this information, the exposure ages from the quarried bedrock were plotted against the time of operation in Figure 8.

## 5. Discussion

In the exposure dating of archaeological surfaces, the most critical difficulty to tackle is the inheritance (e.g., Merchel et al., 2013). This is because of the fact that these surfaces might have been preexposed before quarrying and/or have cosmogenic nuclide concentrations accumulated at depths and thus might constitute a significant amount of inheritance. This potential problem is already known and was apparent in several previous studies, specifically those that dealt with cosmogenic nuclide applications in archaeology (Akçar et al., 2008; Ivy-Ochs and Kober, 2008; Akçar et al., 2009; Merchel et al., 2013; Akçar et al., 2014). Inherited $^{10}$Be concentrations in our samples inhibited the determination of operation periods of the Yedi Taşlar and Zurnacı Değirmeni antique quarries in the Troad. We estimate that the beginning of the excavations was not before the foundation of Alexandria Troas. Based on the radiocarbon ages obtained from charcoal samples from the sediments overlying the ruins of this ancient city, we anticipate the city's demise to have happened between 335 and 395 AD (Figure 7). Therefore, we conclude that these quarries were in operation between 310 BC and 335–395 AD (Figure 8). Exposure ages are older than this interval to the order of thousands of years. Based on results of our field mapping and the 130 kyr minimum exposure age from the natural outcrop in Yedi Taşlar, we estimate that the landscape of the study area is old to the order of at least a few million years. The minimum 130 kyr of exposure is a result of steady-state erosion over a long period of exposure. Applying muonic production of approximately 2% of the surface production at depth (Heisinger et al., 2002a, 2002b) for 150 kyr of exposure, we calculated an inherited $^{10}$Be concentration of at least 1.2 × $10^4$ at/g. This concentration would dramatically increase for exposures on the order of millions of years. Therefore, we conclude that excavation depths of approximately 20 m would be required in old landscapes such as that studied here to successfully date exposures in ancient quarries

**Table 3.** Radiocarbon data of charcoal samples from Alexandria Troas.

| Sample name | ETH code | Material | $^{14}C$ age[a] (BP[b] years) | Delta $^{13}C$ (‰) | Calibrated $^{14}C$ ages (calendar years) |
|---|---|---|---|---|---|
| Talex-1 | ETH-41651 | Charcoal | 1710 ± 35 | –23.1 ± 1.1 | 1s probability<br>AD 250–300 (22.5%)<br>AD 320–390 (45.7%)<br>2s probability<br>AD 240–410 (95.4%) |
| Talex-3 | ETH-43482 | Charcoal | 1680 ± 40 | –23.0 ± 1.1 | 1s probability<br>AD 260–280 (6.4%)<br>AD 330–420 (61.8%)<br>2s probability<br>AD 240–440 (95.4%) |
| Talex-4 | ETH-43483 | Charcoal | 1710 ± 35 | –23.1 ± 1.1 | 1s probability<br>AD 250–300 (22.5%)<br>AD 320–390 (45.7%)<br>2s probability<br>AD 240–410 (95.4%) |
| Talex-5 | ETH-43484 | Charcoal | 1655 ± 35 | –23.0 ± 1.1 | 1s probability<br>AD 340–430 (68.2%)<br>2s probability<br>AD 250–300 (6.5%)<br>AD 320–470 (79.7%)<br>AD 480–540 (9.2%) |
| | Combined $^{14}C$ age | | 1682 ± 21 | - | 1s probability<br>AD 340–405 (68.2%)<br>2s probability<br>AD 260–290 (8.3%)<br>AD 320–420 (87.1%) |

[a] Delta $^{13}C$ corrected radiocarbon age.
[b] BP: Before present (before 1950 AD).
Notes: Delta $^{13}C$ is a value measured on graphite and might include additional fractionation. Radiocarbon ages are calibrated by OxCal 3.1 (https://c14.arch.ox.ac.uk/oxcal; Ramsey, 2005) using the using the atmospheric data from Reimer et al. (2009).

with cosmogenic nuclides. At this point, we consider inheritance as being outside the scope of this study and a methodological issue (e.g., Merchel et al., 2013), and therefore we will not discuss it further.

In ancient times, construction materials were made mainly of sedimentary rocks (e.g., limestones and sandstones), volcanic rocks (e.g., basalts, andesites, ignimbrites, and tuffs), and igneous rocks (e.g., granites). The material available in the surrounding area of the construction site was used first. Sandstones became very popular construction materials due to their softness and simplicity of handling. However, the softness makes sandstones susceptible to weathering and therefore unsuitable for various architectural styles. Similarly, volcanic rocks can be shaped easily owing to their softness; however, these rocks also tend to crack easily. As described by Birkle and Satır (1994), thin sections give an explanation for this behavior. Volcanic rocks usually possess a texture that is formed by isolated phenocrysts embedded in a fine-grained matrix. These phenocrysts lack connections to stabilize the matrix grid, thereby simplifying the opening of cracks in a desired direction. In contrast, igneous rocks such as the Kestanbol quartz-monzonites are densely packed and holocrystalline in texture. Large phenocrystals are intergrown and "cemented" together during slow crystallization. The intergrowth of individual crystals stabilizes the rock, giving it a very strong geotechnical character and enabling the production of supporting parts such as columns in constructions. A major difficulty of a rock besides its hardness is the predetermination

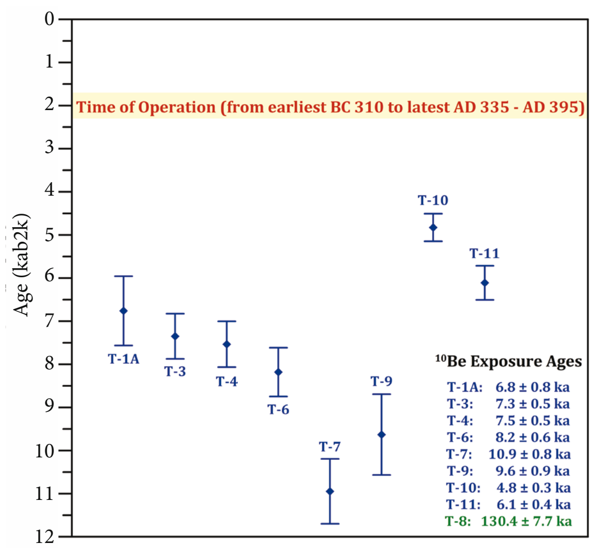


**Figure 8.** Apparent $^{10}$Be exposure ages from the antique quarries in the study area. Note that the beginning of excavations is assumed to be not earlier than the foundation of Alexandria Troas and the end is based on the radiocarbon ages from this study.

of the cleavage direction by the texture, which further complicates the handling (Birkle and Satır, 1994).

Suitable localities for mining blocks of more than 10 m in length are rare within igneous rocks. Birkle and Satır (1994) were convinced that the masons in ancient times had a good understanding of the rock properties and their geotechnical behavior to detect such rare localities like Yedi Taşlar. Factors such as cooling cracks, woolsack weathering (or spheroidal weathering), and tectonic structures reduce the number of potential sites for such high-quality localities. Cooling cracks were formed around the Kestanbol Intrusions when the hot intrusion came into contact with surrounding regions of lower temperature and pressure. The rim of the intrusion cools faster than the center, which causes circular cracks parallel to the lateral shape of the intrusion, comparable with "onion rings". With increase in weathering, such "onion rings" start to peel off and are often combined with woolsack structures. Woolsack structures are common surface features of granitoid rocks or sandstones, altering the rock in the shape of rounded blocks. The tectonic structures vary depending on the direction and magnitude of tectonic stress applied to the rock, but they can usually be detected based on shearing (Birkle and Satır, 1994).

The size of columns in Roman times was standardized, usually multiplied by 4 Roman pedes (singular: pes; 1 Roman pes (foot) = 29.6 cm; Jones, 1989). A common ratio for column diameter to column height was therefore 1:8. Another standard was defined for the length of the shaft (without base and top) to the total length of the column (including base and top) of 5:6. However, not all columns found in buildings were cut according to these rules. The column size in the Roman world varied from large (50 pedes = 14.8 m) to intermediate (approximately 14 pedes = 4.06 m) and small columns. The shaft was usually finished in the quarry itself, but a protective collar of 2–3 cm was left on the top and bottom of the shaft for transport (Barresi, 2002).

Archaeologists have shown in historic reconstructions that the duration of extraction depended on the size of the columns. It took 3 masons from 50 days (a 20-pedes column) to 170 days (a 30-pedes column) to quarry a column. These working days are calculated at 10 working hours a day (DeLane, 1992). The prices for columns and building stones depend on a variety of factors: for example, on the quarried material, the size of the desired column, and the transport distance. A compilation of different price-influencing factors was given by Barresi (2002). For example, to extract a cubic block of 1 m$^3$ of marble (medium hardness) and make it ready for transport (precision work with small chisels), 20 days of work were necessary. One day of work cost 0.5 denarii (singular: denarius; a silver coin in Roman times), so 20 working days amounted to 10 denarii. A pes of, for example, Mons Claudianus granite (a famous quarry in the desert of Egypt, quarried in Roman times) cost in addition 100 denarii. Values for marmor troadense could not be found in the literature.

The extracting techniques and tools for the quarrying of building stones have changed little, in principle, over the last 2000 years. There are dozens of variations of tools used by masons for the extraction and refinement of building stones (Bessac, 1987). Usually some type of hammer and chisel were used for extraction, whereas different rasps, scrapers, and drills were used for refinement. The mason chose his tools according to the stone properties and the desired end product. Each tool left a characteristic mark on the stone (Bessac, 1987).

Once a suitable spot for quarrying was found, the masons removed vegetation and the weathered part of the rocks. Hirt (2010) mentioned that, after cleaning, techniques of broaching or channeling were applied. In these techniques, a channel was created in the rock surface and a line of holes was chiseled in the channels. These channels were usually created perpendicular to the cleavage and joints of the rocks. Metal or wooden wedges were inserted in the holes, which were either hammered or moistened until the stone broke off. To shape the extracted pieces, chisels were used (Hirt, 2010). Ponti (2004) suggested that for the refinement leading to an exact rounding and thinning towards the top, wooden constructions were used. According to Hirt (2010), logistics of undertaking quarries and fabrication was fraught with more difficulties than prospecting and quarrying itself. Skilled and experienced workers had to be assembled and equipped with proper tools. They had to be paid, accommodated (given shelter, food, and water), and supplied with enough raw material (wood, charcoal, iron) to repair or to manufacture the needed tools. For the production of such tools, specialists were required on site (Hirt, 2010). It is not known how many workers and specialists were working in one quarry, but it would have strongly depended on the size of the quarry. Workers were possibly accommodated as close as possible to the quarries, creating worker villages and graveyards around these quarries. Thus, it seems clear that they had to be coordinated by someone (Hirt, 2010).

Once a stone was extracted, it had to be transported over land and sea to its destination. The quarries of valuable stones were not always located in the immediate vicinity of a river or sea enabling a simple transport. In contrary, the stones first encountered an exhausting path over land, roads, and slipways. Therefore, wagons, draught animals, and ships were needed. In some areas, building stones were put on vehicles, which implies the presence of infrastructure (roads and harbors) as well as food and shelter for the animals (Hirt, 2010). Wherever large differences in altitude needed to be conquered, slipways, sleds, rollers, and ropes were built and in some cases cranes were also used. Cranes were furthermore used to lift blocks or columns onto wagons or ships where no loading ramp was available (Bruno, 2002; Hirt, 2010). The extraction needed to be planned in order to ensure that quarrying went on smoothly. The produced rubble from the quarries was deposited at a location where it would not hinder further quarrying while the already extracted stones were being shaped (Hirt, 2010).

Columns are widely distributed in the mapped area (Figure 4). Like all other Roman features, they are not found in the immediate surrounding area of Neandreia. A column of 4 × 0.5 m was mapped on the outer slope of the Granit Türk quarry, implying a Roman excavation located at today's excavation site. The length and thickness of the distributed columns is highly variable, as described above. However, the standard of 1:8 for the length/diameter ratio is only rarely obtained. The reason for the 1:8 ratio not being maintained in our mapping area is not clear. Most columns are in an uncompleted state, making a correct measurement of the final thickness and length impossible. However, several of these columns have a collar on both ends and taper towards the top. It is not fully clear where the columns need to be measured for comparison with Barresi's measurements (Barresi, 2002). Last but not least, some measurements were performed quickly, resulting in a maximum measurement uncertainty of 5 cm. These 3 factors clearly influence the measured length/diameter ratio. However, an error of ±5 cm in the measurement of the length and diameter influences the ratio to a maximum of ±0.4. Therefore, these factors cannot be the sole reason for the deviation from the 1:8 standard. It is also obvious that towards the last period of excavation, possibly in the context of the decay of the Roman Empire, strict rules of producing columns were not maintained anymore, or simply the style of columns changed.

Columns were usually produced within the quarries in the study area and then transported. For this, rasps and scrapers were used with different types of hammers and chisels. Refinement or final ornamentations were most likely completed at the destination construction sites, because there is no evidence for a construction like Ponti (2004) suggested for the refinement of large-sized columns like that at Yedi Taşlar. However, wooden constructions are rarely preserved over long time spans. If such constructions were used, it seems strange that no holes are visible on the bottom of the columns for fixation, which may lead to the use of another type of installation or scaffold. Missing holes to place anchors or handles, as found on columns from Mons Claudianus (Adam, 2010), raise the question of how columns were transported and moved in our study area. Lifting systems with ropes seem to fit best into the picture for putting them on wagons or sleds. The same system was most likely also applied in the harbor of Alexandria Troas. Here also, ramps were used for unloading building stones from the wagons or sleds and for loading them onto ships. During transport, the columns had to be well fixed to prevent them from rolling off the transportation vehicle, which indeed happened, as a lost column along an ancient street towards Alexandria Troas proves.

Based on the remnant columns in the study area, a sudden abandonment of the quarries can be suggested. However, it does not have to be connected to a human or natural catastrophe. Adam (2010) also found similar abandonment in recent quarries, where no successors for the continuation of the business were present. This might also be an explanation for abandoned quarries in the study area. However, it seems bizarre that, throughout this area, several owners abandoned their quarries. The abandonment of quarries appears to be closely linked with the decline of Alexandria Troas.

To give an economic value for the locally produced columns, the following assumptions are made based on DeLane (1992) and Barresi (2002). If we consider a medium-sized column of 20 pedes (5.9 m) in length and 2.2 pedes (0.65 m) in diameter (in total 76 pedes$^3$), according to the 1:8 ratio and 50 days of work for 3 masons, a total cost of 25 denarii is estimated. If 100 denarii per pedes$^3$ is applied to the marmor troadense (same costs of excavation for the Mons Claudianus granite), a sum of 7603 denarii was required for the excavation costs for a 20-pedes column quarried at the Kestanbol Intrusion. DeLane (1992) and Barresi (2002) assumed that its price per pedes[3] and the number of working days for extraction might have been higher due to higher hardness.

Transferring these prices to today's known currencies and wages (assuming 50 euros/day), 350 working hours would cost approximately 17,500 euros. For a medium-sized column of approximately 6 × 0.65 m, 2.5 $m^3$ of rock is needed. Taking the price per $m^3$ for a standard granite to be approximately 100 euros, the material costs for a medium-sized column would be 250 euros. Therefore, a 20-pedes-long column would cost approximately 17,750 euros today. This assumption represents only a minimum value. Transport costs, and adaptation of logistics and machines for the production of 6-m-long columns are not included, as they do not exist anymore in normal factories. For example, the standard blocks in general are no longer than 3 m and machines are usually not designed for longer constructions in a single piece. Therefore, such column productions would need special constructions starting in the quarry, ending in the refinement and placement of the columns, which would increase their price. However, it can also be said that the production costs could be reduced if the columns were produced in Turkey or in China. To summarize, if all 60 columns were intact in our mapped area, they would have a value of 1 to 2 million euros, taking into account that the available columns are 2–3 m in length on average.

Lazzarini (1987) reported scientific investigations of 314 exported quartz-monzonite columns. This number only covers one-fourth of the described export localities. Extrapolating the same number of columns for the remaining three-fourths of localities results in 1270 exported columns. Further extrapolation of the 60 columns found in the 3.7 $km^2$ mapped area to the remaining 80–100 $km^2$ of the Kestanbol Intrusion results in another 1300 to 1620 columns. Thus, calculating the total price for extractions in the Kestanbol Intrusion, based on the price for a medium-sized column and for a total of 2550 to 2870 columns, results in 100 to 150 million euros. Of course, this calculation is a rough estimation, but it indicates the importance of the Kestanbol quartz-monzonite as a building stone.

## 6. Conclusions

This study showed that the Roman quarrying activities took place between 310 BC, when Alexandria Troas was founded, and 365 ± 30 AD based on the calibrated $^{14}C$ age of charcoal fragments from a collapsed part of Alexandria Troas. This age falls in the time span of the last known written record of a visit to the city (Pionius in 452 AD; Ricl, 1997). The quarried steps in Yedi Taşlar seem to be older than similar features from the quarry near Zurnacı Değirmeni, showing ages of 5.2 ± 0.2 ka and 8.6 ± 0.2 ka, respectively. However, all age estimates are too old for being of the Roman period, because inherited $^{10}Be$ concentrations inhibit the surface exposure dating of these quarries. Instead, the evidence for the Roman origin of these quarries is based on field and historic evidence. Minimum landscape ages show that the landscape evolution contains uplift and erosion of over at least 100,000 evolutionary years, adjusting to steady-state erosion.

The detailed map produced in this study clearly suggests that, during Roman times, construction materials were extracted in all areas where their physical properties were good enough. Without any further archaeological investigations, we can only distinguish Roman and non-Roman quarrying activity in the field. Evidence of non-Roman activity can be found in the area immediately surrounding Neandreia, especially in the eastern part, for the Neandreian period. However, Neolithic tools found in this region confirm Schwertheim and Wiegartz's (1994) suggestion that the civilization in this area goes much further back in time than Roman and even Neandreian times. Earlier traces of excavations cannot be found with certainty. However, earlier traces might not be visible anymore due to overprinting activity during Neandreian times and, later, Roman times. Due to the lack of inscriptions throughout the mapped area, features such as fundaments and graveyards cannot be associated with any one civilization with certainty. However, based on Byzantine pottery found on the northern slope of Çığrı Dağ, we can infer that the inhabitants on the slope were trading with Byzantium.

The picture of the remaining columns in the field in various stages of working implies an abrupt abandonment of the quarries. Some possible explanations for the abandonment are siltification of the harbor such that no ship transport was possible anymore, a severe loss of influence due to the declaration of Constantinople as the capital of the Eastern Empire, increasing hostilities as a consequence of the decay of the Western Empire, and/or major earthquakes destroying Alexandria Troas. However, a flourishing and healthy city would not let its harbor fill up with sediment. That means that either the city was already abandoned by the time siltification started or it was already close to complete collapse. The highly disturbed slopes of Çığrı Dağ led to the conclusion that earthquakes played an important role in the study area. However, a combination of all of these factors is more likely to explain the abandonment.

The economic importance of these quarries was enormous, according to extrapolations and comparison with today's value for such columns. A total value of 100 and 150 million euros is estimated for the remnant columns in the quarries and exported columns, without considering the transport costs. Therefore, these quarries were the driving force of the economy for Alexandria Troas.

Quarries hosted many different people in ancient times. Quarrymen, smiths, farmers, builders, and administrative personal were employed around and, in most cases, lived close to the quarries. This might also have been the case for the study area, according to the fundaments close to the quarries. Due to the excellent preservation of the quarries, they represent a unique geoarchaeological heritage site for science that is worth protecting for the future.

**Acknowledgments**
I would like to thank Naki Akçar and Christian Schlüchter at the Institute of Geological Sciences, University of Bern, for their help in the field and in sample preparation for $^{10}$Be analysis. I am grateful to Susan Ivy-Ochs and Vassili Alfimov at the Institute of Particle Physics, ETH, Zurich, for their support in the field. For the $^{10}$Be and $^{14}$C analysis, I am thankful to Peter Kubik and Irka Hajdas at the Zürich AMS Facility operated by the Swiss Federal Institute of Technology, Zürich, Switzerland. I am also grateful to 3 anonymous reviewers for their constructive and helpful comments and suggestions. The digital topographical maps and digital elevation data used in this study were provided by the Turkish General Command of Mapping. This study was funded by İstanbul Technical University (Research Project No. 33245) and the Surface Exposure Dating Laboratory at the University of Bern (Switzerland).

**References**

Adam JP (2010). Roman Building: Materials and Techniques. 1st ed. London, UK: Routledge.

Akarca A (1977). Neandreia: Kuzey Ege'de Arkaik ve Klasik Çağlara ait bir şehir. İstanbul Üniversitesi Edebiyat Fakültesi Yayınları: 2238. 1st ed. İstanbul, Turkey: İstanbul Üniversitesi Edebiyat Fakültesi Matbaası (in Turkish).

Akçar N (2006). Paleoglacial records from the black sea area of Turkey. Field and dating evidence. PhD, University of Bern, Bern, Switzerland.

Akçar N, Ivy-Ochs S, Alfimov V, Yılmaz İÖ, Schachner A, Altıner D, Yavuz V, Schlüchter C (2009). First results on determination of cosmogenic $^{36}$Cl in limestone from the Yenicekale Complex in the Hittite capital of Hattusha (Turkey). Quat Geochronol 4: 533–540.

Akçar N, Ivy-Ochs S, Kubik PW, Schlüchter C (2011). Post-depositional impacts on 'Findlinge' (erratic boulders) and their implications for surface-exposure dating. Swiss J Geosci 104: 445–453.

Akçar N, Ivy-Ochs S, Schlüchter C (2008). Application of in-situ produced terrestrial cosmogenic nuclides to archaeology: a schematic review. J Quaternary Sci 57: 226–238.

Akçar N, Tikhomirov D, Özkaymak Ç, Ivy-Ochs S, Alfimov V, Sözbilir H, Uzel B, Schlüchter C (2012). Cl-36 exposure dating of paleoearthquakes in the Eastern Mediterranean: first results from the western Anatolian Extensional Province, Manisa fault zone, Turkey. Geol Soc Am Bull 124: 1724–1735.

Akçar N, Yavuz V, Ivy-Ochs S, Reber R, Kubik PW, Zahno C, Schlüchter C (2014). Glacier response to the change in atmospheric circulation in the eastern Mediterranean during the Last Glacial Maximum. Quat Geochronol 19: 27-41.

Aldanmaz E, Pearce JA, Thirlwall MF, Mitchell JG (2000). Petrogenetic evolution of late Cenozoic, post-collision volcanism in western Anatolia, Turkey. J Volcanol Geoth Res 102: 67–95.

Altunkaynak S, Genç ŞC (2008). Petrogenesis and time-progressive evolution of the Cenozoic continental volcanism in the Biga Peninsula, NW Anatolia (Turkey). Lithos 102: 316–340.

Balco G, Briner J, Finkel RC, Rayburn JA, Ridge JC, Schaefer JM (2009). Regional beryllium-10 production rate calibration for late-glacial northeastern North America. Quat Geochronol 4: 93–107.

Balco G, Stone JO, Lifton NA, Dunai TJ, (2008). A complete and easily accessible means of calculating surface exposure ages or erosion rates from Be-10 and Al-26 measurements. Quat Geochronol 3: 174–195.

Barresi P (2002). Il Ruolo delle Colonne nel Costo degli Edifici Pubblici. In: Barresi P, editor. Museo dei Fori Imperiali nei Mercati di Traiano. 1st ed. Venice, Italy: Marsilio, pp. 69–81 (in Italian).

Beccaletto L (2003). Geology, correlations, and geodynamic evolution of the Biga Peninsula (NW Turkey). PhD, University of Lausanne, Lausanne, Switzerland.

Bessac JC, (1987). L'outillage traditionnel du tailleur de pierre: De l'antiquité à nos jours. Rev Archéologique de Narbonnaise. Supplément 14. Paris, France: Centre national de la recherche scientifique (in French).

Bingöl E (1976). Evolution geotectonique de l'anatolie de l'oueste. B Soc Geol Fr 18: 431–450 (in French).

Birkle P, Satır M (1994). Geological aspects of the use of Kestanbol quartz- monzonite intrusion (Troas/Turkey) as constructing material in archaeological sites around the Mediterranean Sea. In: Studia Troica. 1st ed. Mainz am Rhein, Germany: Philipp von Zabern, pp. 143–155.

Bozkurt E (2001). Neotectonics of Turkey-a synthesis. Geodyn Acta 14: 3–30.

Bozkurt E, Mittwede SK (2001). Introduction to the geology of Turkey - a synthesis. Int Geo Rev 43: 578-594.

Bruno M (2002). Considerazioni sulle Cave, sui Metodi di Estrazione, di Lavorazione e sui Transporti. In: Museo dei Fori Imperiali nei Mercati di Traiano, editors. I marmi colorati della Roma imperiale. 1st ed. Venice, Italy: Marsilio, pp. 179–193 (in Italian).

Çağlar I, Demirörer M. (1999). Geothermal exploration using geoelectric methods in Kestanbol, Turkey. Geothermics 28: 803–819.

Cassas LF, Le Chevalier JB (1786). Carte de la Troade. Recueil des cartes, plans, vues et medailles pour servir au voyage de la Troade. 1st ed. Paris, France: Dentu (in French).

Chmeleff J, Von Blanckenburg F, Kossert K, Jakob D (2010). Determination of the Be-10 half-life by multicollector ICP-MS and liquid scintillation counting. Nucl Instrum Meth B 268: 192–199.

Choiseul-Gouffier MGFA (1782). Voyage pittoresque de la Grèce. 1st ed. Paris, France: JJ Blaise Libraire (in French).

Clarke JT (1886). A Proto-Ionic capital from the site of Neandreia II. Am J Archaeol 2: 136–148.

Cook JM (1959). Greek archaeology in Western Asia Minor. Archaeol Rep 6: 27–57.

Delaloye M, Bingöl E (2000). Granitoids from Western and Northwestern Anatolia. Geochemistry and modeling of geodynamic evolution. Int Geol Rev 42: 241–268.

DeLane J (1992). Design and construction in Roman Imperial architecture: the baths of Caracalla in Rome. PhD, University of Adelaide, Adelaide, Australia.

Dunne J, Elmore D, Muzikar P (1999). Scaling factors for the rates of production of cosmogenic nuclides for geometric shielding and attenuation at depth on sloped surfaces. Geomorphology 27: 3–11.

Dworakowska A (1983). Quarries in Roman provinces. Bibliotheca antiqua. 16. 1st ed. Wroclaw, Poland: Akademia Nauk.

Errington RM (2008). A History of the Hellenistic World, 323-30 BC. 1st ed. Oxford, UK: Blackwell.

Feuser S (2009). Der Hafen von Alexandria Troas. Asia Minor Studien. 63. 1st ed. Bonn, Germany: Habelt (in German).

Fytikas M, Giuliani O, Innocenti F, Marinelli G, Mazzuoli R (1976). Geochronological data on recent magmatism of the Aegean Sea. Tectonophysics 31: 29–34.

Galetti G, Lazzarini L, Maggetti M (1992). A first characterization of the most important granites used in Antiquity. In: Waelkens M, Herz N, Moens L, editors. Ancient Stones. 1st ed. Leuven, Belgium: Leuven University Press, pp. 167–173.

Gosse JC, Phillips FM (2001). Terrestrial in situ cosmogenic nuclides - theory and application. Quaternary Sci Rev 20: 1475–1560.

Green P (2007). The Hellenistic Age: A Short History. A Modern Library Chronicles Book 27. 1st ed. New York, NY, USA: Modern Library.

Haudenschild E (2011). The Kestanbol Intrusion (Western Turkey) and its importance as a building stone: application of cosmogenic 10Be to archaeology. MSc, University of Bern, Bern, Switzerland.

Heisinger B, Lal D, Jull AJT, Kubik P, Ivy-Ochs S, Knie K, Nolte E (2002a). Production of selected cosmogenic radionuclides by muons: 2. Capture of negative muons. Earth Planet Sc Lett 200: 357–369.

Heisinger B, Lal D, Jull AJT, Kubik P, Ivy-Ochs S, Neumaier S, Knie K, Lazarev V, Nolte E (2002b). Production of selected cosmogenic radionuclides by muons 1. Fast muons. Earth Planet Sc Lett 200: 345–355.

Hirt AM, (2010). Imperial Mines and Quarries in the Roman world: Organizational Aspects, 27 BC-AD 235. Oxford Classical Monographs. Oxford, UK: Oxford University Press.

Ivy-Ochs S, Kober F, (2008). Surface exposure dating with cosmogenic nuclides. J Quaternary Sci 57: 179–209.

Kayan İ (1999). Holocene stratigraphy and geomorphological evolution of the Aegean coastal plains of Anatolia. Quaternary Sci Rev 4-5: 541–548.

Kohl CP, Nishiizumi K (1992). Chemical isolation of quartz for measurement of *in-situ*-produced cosmogenic nuclides. Geochim Cosmochim Ac 56: 3583–3587.

Korschinek G, Bergmaier A, Faestermann T, Gerstmann UC, Knie K, Ruge, G, Wallner A, Dillmann I, Dollinger G, Von Gostomski CL et al. (2010). A new value for the half-life of Be-10 by heavy-ion elastic recoil detection and liquid scintillation counting. Nucl Instrum Meth B 268: 187–191.

Koldewey R (1891). Neandria. Programm zum Winckelmannsfest der Archäolo-gischen Gesellschaft zu Berlin 51. Berlin, Germany: Druck & Verlag Georg Reimer (in German).

Kubik PW, Christl M (2010). $^{10}$Be and $^{26}$Al measurements at the Zurich 6 MV Tandem AMS facility. Nucl Instrum Meth B 268: 880–883.

Lazzarini L (1987). I Graniti dei Monumenti Italiani e i loro Problemi di Deterioramento. In: Bueca A, Tabasso ML, editors. Materiali lapidei: problemi relativi allo studio del degrado e della conservazione. 1st ed. Rome, Italy: Zecca dello Stato, pp. 157–173 (in Italian).

Lazzarini L (2002). La determinazione della provenienza delle pietre decorative usate dai Romani. In: Ungaro L, Nuccio M, editors. I marmi colorati della Roma imperiale. 1st ed. Rome, Italy: Marsilio, pp. 233–268 (in Italian).

Merchel S, Braucher R, Alfimov V, Bichler M, Bourles D, Reitner JM (2013). The potential of historic rock avalanches and man-made structures as chlorine-36 production rate calibration sites. Quat Geochronol 18: 54–62.

Mützenberg SR (1991). Westliche Biga-Halbinsel (Canakkale, Türkei), Beziehung zwischen Geologie, Tektonik und Entwicklung der Thermalquellen. PhD, ETH, Zürich, Switzerland (in German).

Okay A, Tüysüz O (1999). Tethyan sutures of northern Turkey. Geol S Am S 156: 475–515.

Pensabene P (2002). Il Fenomeno del Marmo nel Mondo Romano. In: Museo dei Fori Imperiali nei Mercati di Traiano, editors. I marmi colorati della Roma imperiale. 1st ed. Venice, Italy: Marsilio, pp. 3–67 (in Italian).

Philippson A (1918). Kleinasien. In: Steinmann G, Wilckens O, editors, Handbuch der Regionalen Geologie. 1st ed. Heidelberg, Germany: C Winter (in German).

Pococke R (1743–1745). A Description of the East and Some Other Countries, Vol. 2. 1st ed. London, UK: W Bowyer.

Ponti G (1995). Marmor troadense-granite quarries in the Troad. A preliminary survey. In: Studia Troica 5. Mainz am Rhein, Germany: Phillip von Zabern, pp. 291–320.

Ponti G (2002). Tecniche di Estrazione e di Lavorazione delle Colonne Monolitiche di Granito Troadense. In: Museo dei Fori Imperiali nei Mercati di Traiano, editors. I marmi colorati della Roma imperiale. 1st ed. Venice, Italy: Marsilio, pp. 291–295 (in Italian).

Reimer PJ, Baillie MGL, Bard E, Bayliss A, Beck JW, Blackwell PG, Ramsey CB, Buck CE, Burr GS, Edwards RL et al. (2009). IntCal09 and Marine09 radiocarbon age calibration curves, 0-50.000 years cal BP. Radiocarbon 51: 1111–1150.

Ricl M (1997). The inscriptions of Alexandreia Troas. Inschriften griechischer Städte aus Kleinasien 53. Bonn, Germany: Habelt.

Savaşçın MY, Güleç N (1990). Relationship between magmatic and tectonic activities in Western Turkey: geological and geochemical features with examples from the coastal section. In: Savaşçın MY, Eronat AH, editors. IESCA 1990 Proceedings. İzmir, Turkey: International Earth Science Colloquium on the Aegean Region, pp. 300–313.

Schliemann H (1881). Reise in der Troas im Mai 1881. 1st ed. Leipzig, Prussia: FA Brockhaus (in German).

Schulz A (2000). Die Stadtmauern von Neandreia in der Troas. Asia-Minor-Studien 38. Bonn, Germany: Rudolf Habelt (in German).

Schwertheim E, Wiegartz H (1994). Neue Forschungen zu Neandria und Alexandria Troas. Asia Minor Studien 11. 1st ed. Bonn, Germany: Rudolf Habert (in German).

Şengör AMC, Yılmaz Y (1981). Tethyan evolution of Turkey: a plate tectonic approach. Tectonophysics 75: 181–241.

Seyitoğlu G, Scott BC (1996). The cause of N-S extensional tectonics in western Turkey: tectonic escape vs back-arc spreading vs orogenic collapse. Geodynamics 22: 145–153.

Spühler M (1991). Die Kestanbol-Intrusion und ihre Vererzungen: Geologische, Petrologische und Isotopengeochemische Aspekte westliche Biga-Halbinsel (Türkei). MSc, ETH, Zürich, Switzerland (in German).

Taşçı MA (2010). Alexandreia Troas. Am J Archaeol: 168–185.

Virchow R (1879). Beiträge zur Landeskunde der Troas. Berlin, Prussia: Abhandlungen der Preussischen Akademie der Wissenschaften. Physikalisch-Mathematische Classe 3.

Waelkens M (1992). Bronze age quarries and quarrying techniques in the Eastern Mediterranean and the Near East. In: Herz N, Waelkens M, Moens L, editors. Ancient Stones: Quarrying, Trade and Provenance. 1st ed. Leuven, Belgium: Leuven University Press, pp. 5–21.

Williams-Thorpe O (2008). A thousand and one columns: observations on the Roman granite trade in the Mediterranean area. Oxford J Archaeol 27: 73–89.

Wilson Jones M (1989). Designing the Roman Corinthian order. J Roman Stud 2: 35–69.

Winter FE (1985). Notes on Neandria. Am J Archaeol 89: 680–683.

Yılmaz Y, Karacık Z (2001). Geology of the northern side of the Gulf of Edremit and its tectonic significance for the development of the Aegean grabens. Geodyn Acta 14: 31–43.